



Simulation of solute transport across low-permeability barrier walls

Philip T. Harte^{a,*}, Leonard F. Konikow^b, George Z. Hornberger^b

^a *U.S. Geological Survey, Pembroke, NH 03275, United States*

^b *U.S. Geological Survey, Reston, VA 20192, United States*

Received 23 December 2004; received in revised form 24 January 2006; accepted 5 February 2006

Available online 5 April 2006

Abstract

Low-permeability, non-reactive barrier walls are often used to contain contaminants in an aquifer. Rates of solute transport through such barriers are typically many orders of magnitude slower than rates through the aquifer. Nevertheless, the success of remedial actions may be sensitive to these low rates of transport. Two numerical simulation methods for representing low-permeability barriers in a finite-difference groundwater-flow and transport model were tested. In the first method, the hydraulic properties of the barrier were represented directly on grid cells and in the second method, the intercell hydraulic-conductance values were adjusted to approximate the reduction in horizontal flow, allowing use of a coarser and computationally efficient grid. The alternative methods were tested and evaluated on the basis of hypothetical test problems and a field case involving tetrachloroethylene (PCE) contamination at a Superfund site in New Hampshire. For all cases, advective transport across the barrier was negligible, but preexisting numerical approaches to calculate dispersion yielded dispersive fluxes that were greater than expected. A transport model (MODFLOW-GWT) was modified to (1) allow different dispersive and diffusive properties to be assigned to the barrier than the adjacent aquifer and (2) more accurately calculate dispersion from concentration gradients and solute fluxes near barriers. The new approach yields reasonable and accurate concentrations for the test cases.

Published by Elsevier B.V.

Keywords: Barrier wall; Low permeability; Dispersion; Solute transport

* Corresponding author. Tel.: +1 603 226 7813; fax: +1 603 226 7894.

E-mail address: ptharte@usgs.gov (P.T. Harte).

1. Introduction

Low-permeability, non-reactive, barrier walls are used to contain contaminants in an aquifer and prevent further spreading of contaminants in groundwater. There are several types of barrier walls including slurry-trench walls, grout curtains, and sheet piling cutoff walls (Knox et al., 1984). Slurry-trench wall barriers, which are the focus of this study, are constructed of low-permeability materials that are less permeable than the surrounding aquifer they are inserted into. These barriers are not impermeable, however, and some solute transport occurs through them, although at rates that are much slower than rates of solute transport in the aquifer.

Barriers are typically used in conjunction with interior and exterior extraction wells to help maximize containment inside the barrier and capture leakage outside the barrier (U.S. Environmental Protection Agency, 1996). Interior extraction wells are used with barriers to insure inward hydraulic gradients and to remove contaminants inside the barrier. Exterior extraction wells are used to help capture leakage that has been transported through the barrier, on the downgradient side of the barrier, and to remove contaminants outside of the barrier. Extraction wells locally steepen hydraulic gradients, which can increase advective velocities near and through a barrier wall.

Accurate calculation of rates of solute transport through a barrier wall is important for evaluating remedial activities and determining the time needed to restore an aquifer. Inaccuracies in such calculations can impact results of a simulation, and perhaps lead to non-optimal remedial actions. For example, simulation results that show a difference of a few parts per million in solute transport through a barrier may lead to decisions that prompt different outcomes in remedial design or operation. Overpredicting solute flux through the barrier will exaggerate solute concentrations outside of the barrier and may result in an inappropriate design of a remedial system or inaccurate forecasting of operational times of remedial wells. Underpredicting solute flux will result in the forecasting of overly optimistic clean-up times and also affect the proposed design or operation of remedial wells. Therefore, care must be taken to assure that appropriate and accurate simulation methods are used to best reflect field conditions.

Among the commonly used finite-difference simulation approaches, there are a variety of numerical methods that can be used to represent low-permeability barriers, and consequently, result in a variety of solutions and ranges of results. The two primary methods are direct and indirect representations of the barrier. In the direct method, the hydraulic properties and physical dimensions of the barrier are represented directly by the properties assigned to the grid cells coinciding with the location of the barrier within the aquifer. Because barriers are usually narrow relative to the scale of the groundwater-flow system, this approach may require the use of a very fine grid. Because it is often necessary to simulate groundwater flow on a regional scale in order to accurately compute the changes in head that control transport at a local or site scale, direct representation of a barrier may be computationally expensive. If the barrier width is small relative to the horizontal dimensions of cells in the grid, then the indirect method offers a reasonable and computationally efficient approach. In the indirect method, the hydraulic properties of the barrier are represented indirectly by adjusting the intercell hydraulic conductance, for cell faces coinciding with the barrier location, to represent primarily the properties of the barrier rather than the properties of the adjacent cells, which are assigned aquifer properties. The indirect method is described by Hsieh and Freckleton (1993) and has the advantage that it does not require discretization of the model to accommodate the dimensions of the barrier, and can be used with a relatively coarse model grid.

Neville et al. (1998) noted deficiencies in numerical simulation of solute transport through indirectly represented low-permeability features, including barriers formed by constructed slurry walls. The results of their numerical experiments comparing direct and indirect representations indicated that the indirect representation yielded premature breakthrough and solute-flux rates through the barrier that were too high. They attribute these errors to the inherent inability of the indirect representation to simulate either solute storage or transport distance and travel time in the barrier because the barrier width is assumed to be infinitesimally small. Their numerical experiments and analysis, however, used standard finite-difference approximations to estimate concentration gradients and assumed uniform transport properties. That is, the same dispersivities and effective diffusion coefficients apply to transport across the barrier as to transport through the aquifer.

The purpose of this study is to develop a reliable means to simulate solute transport through low-permeability barriers when the groundwater-flow equation is solved using an indirect representation of the barrier. We develop an improved method to estimate local concentration gradients near a barrier wall and allow unique transport properties to be assigned to the barrier material. This paper describes results of numerical simulation tests to assess alternative methods for simulating solute transport through a low-permeability, non-reactive barrier wall. The applicability of the methodology to real-world problems is demonstrated through the simulation of an observed tetrachloroethylene (PCE) plume at a Superfund site in New Hampshire where a barrier wall has been constructed.

2. Numerical models

2.1. Groundwater-flow model

Simulations of groundwater flow used the U.S. Geological Survey MODFLOW model (McDonald and Harbaugh, 1988; Harbaugh and McDonald, 1996; Harbaugh et al., 2000). MODFLOW is a commonly used model for simulating three-dimensional groundwater-flow systems. MODFLOW uses implicit, block-centered, finite-difference methods to numerically solve the governing three-dimensional groundwater flow equation. In developing the finite-difference equations, the flux between adjacent cells of the finite-difference grid is usually computed on the basis of the harmonic mean of the hydraulic conductivities at the two adjacent nodes. The fluid flux between two nodes (that is, across a cell face) is computed on the basis of the hydraulic conductance and the difference in head between those two nodes. The hydraulic conductance between two cells, called the branch conductance, is related to the mean hydraulic conductivity and the distance between the nodes. For example, the branch conductance in the row (or x) direction between two adjacent cells (e.g., cells j,i and cell $j+1,i$; Fig. 1) in a given grid layer can be represented, following McDonald and Harbaugh (1988, chap. 5, pp. 6, Eq. (38), and pp.7, Fig. 25), but using the cell indexing notation of Konikow et al. (1996), as:

$$\frac{1}{CR_{j+1/2,i}} = \frac{1}{\frac{TR_{j,i}\Delta y_i}{\Delta x_j}} + \frac{1}{\frac{TR_{j+1,i}\Delta y_i}{\Delta x_{j+1}}} \quad (1)$$

where $CR_{j+1/2,i}$ is the branch conductance in the row direction between nodes j,i and $j+1,i$ [L^2T^{-1}]; $TR_{j,i}$ is the transmissivity in the row (or x) direction of the indicated cell [L^2T^{-1}]; Δx_j is the grid spacing in the row (or x) direction of column j [L]; and Δy_i is the grid spacing

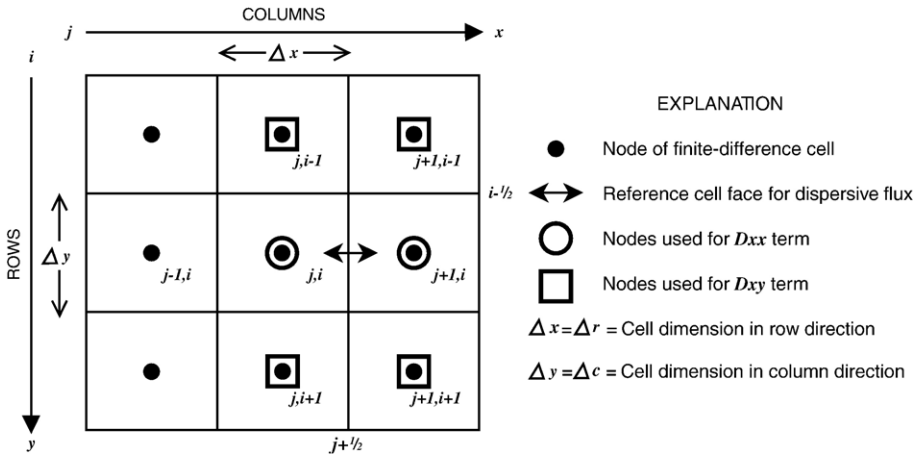


Fig. 1. Representative cells in a block-centered, finite-difference grid showing notation used to label rows, columns, and nodes used in calculating concentration gradients at $(j + 1/2, i)$ (modified from Konikow et al., 1996).

in the column (or y) direction of row i [L]. Note that for simplicity, and because we only need to describe horizontal fluxes for the purposes of this analysis, we drop the index for the layer (or z) direction in all terms.

A method was developed by Hsieh and Freckleton (1993) that allows MODFLOW to more efficiently simulate thin, vertical, low-permeability geologic or artificial features that impede horizontal flow of groundwater. This method was incorporated into MODFLOW as an optional package called the Horizontal-Flow Barrier (HFB) Package. Thin vertical features are approximated by assigning appropriately low hydraulic-conductance values to the face between two contiguous model cells where the barrier is located. The key assumptions in the use of the HFB Package are that the width of the barrier is negligibly small relative to the horizontal spacing of the adjacent model cells and that there is no storage capacity within the barrier materials. In the presence of a horizontal flow barrier, the branch conductance in the row (or x) direction can be expressed as:

$$\frac{1}{CR_{j+1/2,i}} = \frac{1}{\frac{TR_{j,i}\Delta y_i}{\frac{\Delta x_j}{2}}} + \frac{1}{TDW_{j+1/2,i}\Delta y_i} + \frac{1}{\frac{TR_{j+1,i}\Delta y_i}{\frac{\Delta y_{j+1}}{2}}} \tag{2}$$

where $TDW_{j+1/2,i}$ is the barrier transmissivity divided by the width of the barrier between cells j, i and $j + 1, i$ [LT^{-1}]. Because the method directly modifies the intercell or branch hydraulic conductance (Eq. (1)), the barrier width is not explicitly represented in the solution; it is indirectly represented by the TDW term in Eq. (2).

2.2. Solute-transport model

Simulations of solute transport used the U.S. Geological Survey MODFLOW-GWT model (formerly called MOC3D) (Konikow et al., 1996). MODFLOW-GWT is an optional simulation process for the MODFLOW model that solves the three-dimensional solute-transport equation. The solute-transport equation describes changes in concentration over time

caused by processes of advection, dispersion, fluid sources, retardation, and decay, and may be written as:

$$\frac{\partial C}{\partial t} + \frac{V_i}{R_f} \frac{\partial C}{\partial x_i} - \frac{1}{\varepsilon R_f} \frac{\partial}{\partial x_i} \left(\varepsilon D_{ij} \frac{\partial C}{\partial x_j} \right) - \frac{\sum [W(C'-C)]}{\varepsilon R_f} + \lambda C = 0 \quad (3)$$

where C is volumetric concentration (mass of solute per unit volume of fluid, ML^{-3}), ε is the effective porosity (dimensionless), V is a vector of interstitial fluid velocity components (LT^{-1}), D is a second-rank tensor of dispersion coefficients (L^2T^{-1}), W is a volumetric fluid sink ($W < 0$) or fluid source ($W > 0$) rate per unit volume of aquifer (T^{-1}), C' is the volumetric concentration in the sink/source fluid (ML^{-3}), λ is the decay rate (T^{-1}), R_f is the retardation factor (assuming a linear equilibrium sorption isotherm), t is time (T), and x_i are the Cartesian coordinates (L). Summation over repeated indices is understood.

The third term in Eq. (3) represents the change in concentration due to hydrodynamic dispersion. This conventional Fickian model assumes that the driving force is the concentration gradient and that the dispersive flux occurs in a direction from higher toward lower concentrations. The dispersion coefficient may be related to the velocity of groundwater flow and defined in terms of the longitudinal and transverse dispersivities, α_L and α_T , as:

$$D_{ij} = (\alpha_L - \alpha_T) \frac{V_i V_j}{|V|} + (d^* + \alpha_T |V|) \delta_{ij} \quad (4)$$

where d^* is the effective coefficient of molecular diffusion (L^2T^{-1}); V_i and V_j are components of the velocity vector in the i and j directions, respectively; $|V|$ is the magnitude of velocity; and $\delta_{ij} = 1$ if $i = j$ and $\delta_{ij} = 0$ if $i \neq j$. Where horizontal groundwater flow is parallel to a low-permeability barrier wall, one of the velocity components approaches zero, and the mechanical dispersive flux should also approach zero. However, velocity components at finite-difference nodes adjacent to a barrier will be nonzero if (1) there is a regional hydraulic gradient across the barrier, (2) injection or extraction wells operate close to the barrier, or (3) the barrier is not aligned with the grid.

MODFLOW-GWT numerically solves the transport equation using various operator splitting techniques in which the advective terms are solved separately from the terms representing dispersive fluxes. One approach uses the method of characteristics, as described by Konikow et al. (1996) and Kipp et al. (1998). A second approach uses a finite-volume Eulerian–Lagrangian localized adjoint method (Heberton et al., 2000). In all cases, the transport solver uses the heads and groundwater fluxes computed by MODFLOW to calculate the velocity of groundwater.

Because hydraulic conductivity is a property of the porous media, the cross-product terms of the conductivity tensor drop out of the governing flow equation that is solved in a model by aligning the model grid with the major axes of the hydraulic-conductivity tensor. This common assumption simplifies the flow equation used in finite-difference models. This same simplification, however, typically is not possible for the dispersion tensor in the transport equation because the dispersion tensor is also related to, and depends on, the flow direction, which changes orientation over space and time. In general, it is not possible to design a fixed grid that will always be aligned with a changing flow field. Therefore, solute-transport models must evaluate the cross-product terms of the dispersion tensor.

Applying finite-difference approximations that are centered-in-space and explicit, the component of the dispersive flux in the x -direction across the cell face at $(j+1/2, i)$ due to concentration gradients in the x - and y -directions, for example, may be written as:

$$-\left(\varepsilon b D_{xm} \frac{\partial C}{\partial x_m}\right)_{j+1/2, i} = -(\varepsilon b D_{xx})_{j+1/2, i} \frac{(C_{j+i,1} - C_{j,i})}{\Delta x} - (\varepsilon b D_{xy})_{j+1/2, i} \frac{(C_{j,i+1} + C_{j+1,i+1} - C_{j,i-1} - C_{j+1,i-1})}{4\Delta y} \quad (5)$$

To simplify this discussion, Eq. (5) is presented in a form that assumes that both Δx and Δy are constant (Fig. 1).

The first term on the right side of Eq. (5) includes a principal component of the dispersion tensor (D_{xx}) and describes the dispersive flux of solute in the x -direction (that is, across the cell face at $j+1/2$) due to concentration gradients in the x -direction. The concentration gradient associated with this term is estimated simply and directly from the difference in concentration at the adjacent nodes ($j+1, i$ and j, i) divided by the distance between them (Δx). The cross-product coefficient (D_{xy}) in the second term on the right side of Eq. (5) controls the dispersive flux in the x -direction caused by a concentration gradient in the y -direction. A lower order of accuracy, however, is associated with the estimation of the corresponding concentration gradient because the concentration gradient in the y -direction cannot be computed directly at the $j+1/2$ location. Instead, for the D_{xy} term, the best approximation for $\partial C/\partial y$ at $j+1/2$ involves averaging the estimates of $\Delta C/\Delta y$ at the two adjacent nodes ($j+1, i$ and j, i), both of which must be calculated over distances of twice the grid spacing.

These finite-difference approximations work well if the concentration field is smoothly varying over the area of a few grid cells and are consistent with an assumption that concentrations vary linearly between adjacent nodes of the grid. Where an artificial barrier has been constructed, the assumption of locally smooth concentration changes may not be applicable as the barrier is designed to contain solute transport. Therefore, abrupt changes in concentration may occur from one side of the barrier to the other and concentration differences across the barrier may not be indicative of local concentration gradients on both sides of the barrier. The implication of this for the numerical methods is illustrated in Fig. 2, which shows a barrier coinciding with $i-1/2$ (that is, aligned with the cell faces between row i and row $i-1$ in the grid). In this example, the barrier separates an area where the groundwater has relatively high concentrations ($C=100$) in rows i and $i+1$ from an area having low concentrations ($C=1$) in row $i-1$. Within the “contaminated” zone south of the barrier there should be no dispersive flux in the x -direction across $j+1/2$ driven by the concentration gradient in the x -direction because the concentration gradient at $j+1/2$ is zero. Also within the “contaminated” zone south of the barrier, the concentrations are uniform and the gradient in the y -direction is also zero (which implies that the concentration gradient occurs within the barrier material). So across the cell face at $j+1/2, i$, there should also be no dispersive flux in the x -direction caused by a concentration gradient in the y -direction. But if we apply the standard finite-difference approximations for the cross-product terms (Eq. (3)), the result is a nonzero concentration gradient in the y -direction at $j+1/2, i$ as $\partial C/\partial y \approx (1-100)/2\Delta y = -49.5/\Delta y$. Consequently, solute flux will be computed erroneously across the cell face at $j+1/2, i$ if velocities are nonzero.

A reasonable solution to this numerical problem can be derived by assuming that in the presence of a barrier, the concentration gradient immediately adjacent to one side of the barrier

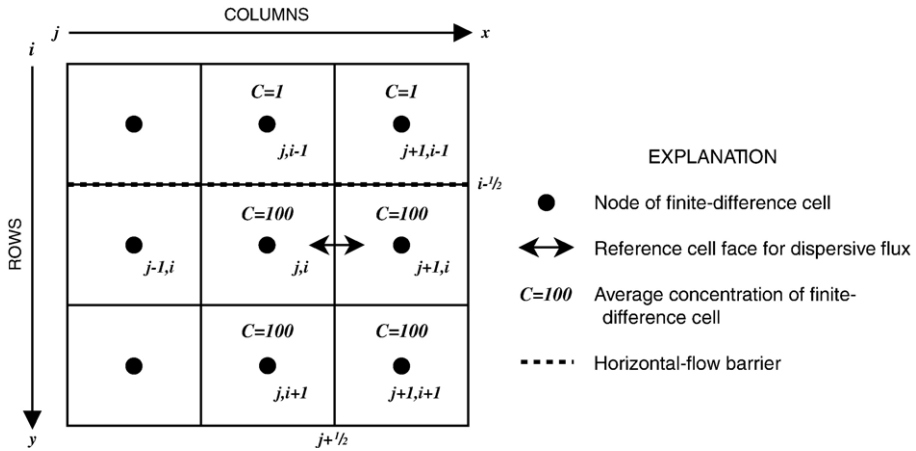


Fig. 2. Hypothetical concentration values at cells used to estimate concentration gradients for calculating dispersive solute flux in x -direction (across cell face at $j + 1/2, i$) due to gradient in y -direction for example case in which a barrier is aligned with cell faces at $i - 1/2$.

should be estimated only on the basis of differences in nodal concentrations on the same side of the barrier. For example, in the case illustrated in Fig. 2, $(\partial C / \partial y)_{j,i} \approx (C_{j,i+1} - C_{j,i}) / \Delta y$, which is equivalent to assuming that $(\partial C / \partial y)_{j,i} \approx (\partial C / \partial y)_{j,i+1/2}$. Modifying Eq. (5) for this approximation allows us to write the term for the dispersive flux in the x -direction due to a concentration gradient in the y -direction as:

$$-\left(\epsilon b D_{xy} \frac{\partial C}{\partial x_y} \right)_{j+1/2,i} = -(\epsilon b D_{xy})_{j+1/2,i} \frac{(C_{j,i+1} + C_{j+1,i+1} - C_{j,i} - C_{j+1,i})}{2\Delta y} \tag{6}$$

The assumption represented by Eq. (6) for the D_{xy} term of the dispersion tensor, and an analogous expression for the D_{yx} term, have been incorporated into a revised version of the MODFLOW-GWT model through the new CHF B Package, as discussed and documented by Hornberger et al. (2002). In this new code, a check is performed to see if a cell is adjacent to a barrier, as represented in the HFB Package. If it is, then the horizontal concentration gradients used to calculate the cross-product dispersive flux of solute in the horizontal plane are estimated using modified finite-difference formulations, as in Eq. (6).

To be consistent with the assumption that the barrier wall has hydraulic properties different from that of the aquifer, the transport properties of the barrier may also be different from those of the adjacent aquifer. The original MODFLOW-GWT model allows the user only to specify unique values of the dispersivity coefficients in each layer, but not spatially varying values. It also allows a single constant and uniform value to be specified for an effective coefficient. Therefore, the capability to assign unique dispersivity (α_L and α_T) and effective diffusion coefficient (d^*) values for the properties of the barrier was incorporated into the new CHF B Package. Then, for cells adjacent to a barrier, such as $j, i - 1$ and j, i in Fig. 2, the dispersion coefficients on the cell face corresponding with the location of the barrier would be computed by solving Eq. (2) using barrier values for α_L , α_T , and d^* rather than aquifer values for these parameters.

3. Methods of simulation

This study aims to develop and assess improved methods to simulate solute transport in the presence of low-permeability barriers with existing numerical models. Evaluation of the results of alternative methods to represent the barriers will be used to decide whether existing methods are adequate and which approach best simulates solute transport. Two test cases were selected for their relevancy to this problem.

The two test cases evaluated included (1) a hypothetical simplified example of a barrier wall and (2) a field case from a Superfund site. The hypothetical example is patterned after the field case but it is simplified to more easily modify model input to test various simulation methods and to observe changes in results.

The two principal simulation methods tested included directly specifying the hydraulic properties of the low-permeability barrier within the aquifer and indirectly representing the barrier with the use of the HFB Package of MODFLOW. The direct representation of the barrier was tested only in the hypothetical example. During initial testing, it became apparent that the principal mechanism of solute transport across the barrier was from dispersion, which prompted the modification and enhancement of the MODFLOW-GWT code (Eq. (6)) to more accurately simulate dispersion across barriers.

Direct representation of the barrier requires that the hydraulic properties of the barrier be included in the assigned properties of the simulated aquifer. In a discretized numerical model, the hydraulic properties of the barrier are assigned to the model cells where the barrier is located. If the barrier width is smaller than the model cell width, an equivalent hydraulic property must be used that maintains the proportional widths of the aquifer and barrier relative to the model cell width.

A simple method of assigning an equivalent hydraulic conductivity, which combines the hydraulic conductivity of the barrier and the hydraulic conductivity of the aquifer, is to compute the harmonic mean from the hydraulic conductivity of the aquifer and barrier. The equivalent harmonic mean hydraulic conductivity can be computed from the equation:

$$K_{eq} = (L_a + L_b) / ((L_a/K_a) + (L_b/K_b)) \quad (7)$$

where K_{eq} is the equivalent hydraulic conductivity, L_a is the width of aquifer in the model cell, L_b is the width of the barrier in the model cell, K_a is the hydraulic conductivity of aquifer, and K_b is the hydraulic conductivity of the barrier.

The harmonic mean is suitable as a representative hydraulic conductivity for conditions where the hydraulic conductivity field is abrupt and discontinuous—conditions occur between the aquifer and barrier. The harmonic mean provides values of equivalent hydraulic conductivity that are weighted toward the lowest hydraulic conductivity value and will tend to be similar to the barrier hydraulic conductivity under certain conditions.

The ratio of the computed equivalent hydraulic conductivity (K_{eq}) to the barrier hydraulic conductivity (K_b) can be related to the ratio of wall width (L_b) to cell width ($L_a + L_b$). For an example in which $K_a = 5 \times 10^2$ and $K_b = 1.42 \times 10^{-4}$ ft/day, this relation is represented by the dimensionless plot shown in Fig. 3. For the values presented in the dimensionless plot, the aquifer hydraulic conductivity (K_a) is more than six orders of magnitude greater than the hydraulic conductivity of the barrier, the barrier width is varied from 1 to 25 ft (ranges typical of barrier wall widths), and the cell width is kept constant at 25 ft. The plot shows that there is an exponential relation between the computed equivalent horizontal hydraulic conductivity (as a multiple of the

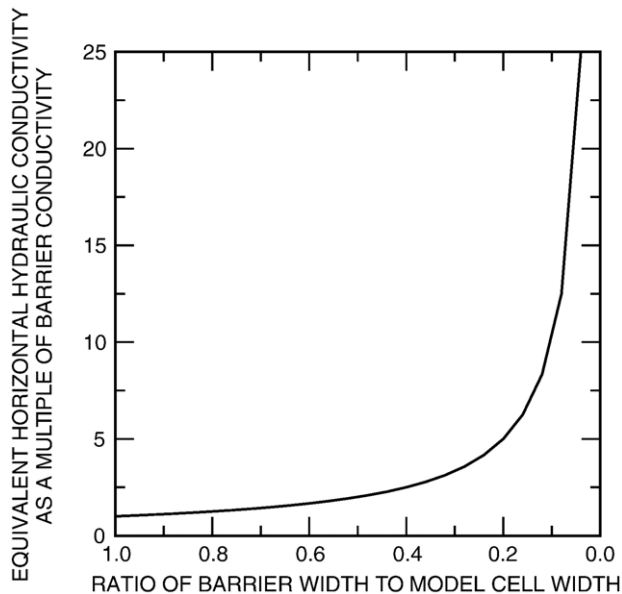


Fig. 3. Equivalent horizontal hydraulic conductivity as a function of barrier wall width to model cell width and barrier horizontal hydraulic conductivity.

barrier horizontal hydraulic conductivity) and the relative dimensions (ratio) of the barrier width to the model cell width.

As the barrier width becomes increasingly small relative to the cell width, the equivalent hydraulic conductivity sharply increases relative to the hydraulic conductivity of the barrier. Differences are small between the equivalent hydraulic conductivity and the hydraulic conductivity of the barrier for large ratios, but differences are large for small ratios (less than half the width of the cell). Therefore, simulations using the direct representation method will poorly represent the hydraulic conductivities of the barrier if the model discretization is too coarse relative to the barrier width because the computed equivalent hydraulic conductivity will be too large.

The dimensions of the barrier wall also play a role in the adequacy of the indirect method to accurately represent the barrier. In contrast to the direct method, the indirect method will provide more accurate representation when the actual barrier wall is thin. As the width increases, the indirect method will overpredict the rate of solute transport through the barrier because it excludes the physical dimensions (width) of the barrier in the solute-transport equation (Eq. (3)).

4. Overview of test cases

Several test problems were used to evaluate and demonstrate the value and accuracy of the new approach, and two are described in more detail in this paper. One basic test problem (only summarized herein for brevity) was designed to demonstrate the efficiency and accuracy of the new approach and is described in detail in Konikow et al. (2001) and Hornberger et al. (2002). These tests used a fine grid (where the model cell width equals the barrier width) to explicitly represent a barrier that is aligned with the grid and a coarse grid (where cell width is three times wider than the barrier width) to evaluate results. Results of this direct representation of the barrier

were compared with simulations in which the barrier is represented indirectly, both using the same fine and coarse grids. The results showed that simulating solute transport without the modifications described in this paper substantially overestimated the dispersive solute flux through the barrier, but that using the new method to estimate concentration gradients near a barrier and specifying unique transport properties for the barrier (1) essentially eliminated artificial upstream dispersion on the upstream side of the barrier, (2) reduced the dispersive flux across the downstream side of the barrier, and (3) yielded good results when the grid was coarsened by a factor of three in each direction (which improved efficiency by reducing the run time for the simulation by a factor of about 100).

Two transport test problems described in this paper include (1) a hypothetical example of two-dimensional (2D) transport of PCE through an irregularly shaped barrier and (2) a field case of three-dimensional (3D) transport of PCE at a Superfund site with a constructed low-permeability barrier wall. Both examples assume the barrier is comprised of a low-permeability slurry. Solute transport and hydraulic properties of the hypothetical example are based on the field case, but simplified to enable isolation of controlling factors. Simulations of transient transport of PCE are made assuming that PCE transport is subject to retardation ($R_f=2.5$), and longitudinal and transverse dispersivities were set at 54 and 12 ft, respectively. For the 3D field case, vertical transverse dispersivities were set at 1/10th the horizontal transverse dispersivity, or 1.2 ft.

The flow system in the hypothetical example represents a simplified steady state version of the transient flow field case that eliminates the complex series of remedial injection and extraction wells operational in the field case and represented in its simulation. However, the major features of the two flow systems are similar, including the ambient horizontal hydraulic gradients, at about 0.014 ft/ft, and the primary horizontal groundwater-flow directions from west to east. This simplification of the field case allows us to examine the effects related to a non-rectangular barrier geometry, which cannot be aligned with the grid because of its irregular shape.

The hydraulic conductivities differ slightly in the transport examples in that the simulated system is homogeneous and isotropic in the hypothetical example but heterogeneous and anisotropic in the field case. Hydraulic conductivity was set at 500 ft/day in the hypothetical example, and varied from 15 to 450 ft/day horizontally and 4 to 112 ft/day vertically for the field case. In both cases we assumed $\epsilon=0.3$ and $d^*=0.0$.

The hydraulic properties of the barrier wall were set at values reported from the field case. The hydraulic conductivity of the barrier was set at 1.42×10^{-4} ft/day, more than six orders of magnitude less than the aquifer, based on reported permeability tests of the slurry used in constructing the barrier wall (Peter J. Borowiec, Jr., 1998). Porosity of the simulated wall was constant at 0.30. The barrier width is 3 ft in both examples. Model cells are square in the hypothetical example with a width and length of 25 ft. Model cells are rectangular in the field case with a width and length of 25 and 50 ft, respectively. As a result, the areal percentage of the cell occupied by the barrier differs slightly in the two examples. In both cases the barrier wall occupies about 10% of the cell area, although the occupied area varies a few percent depending on the orientation of the barrier to the grid.

5. Hypothetical test problem

5.1. Description

The transport domain is shown in Fig. 4. The 2D finite-difference model includes 532 cells with a uniform grid spacing of 25 ft. The domain is 475 ft wide in a north–south direction and

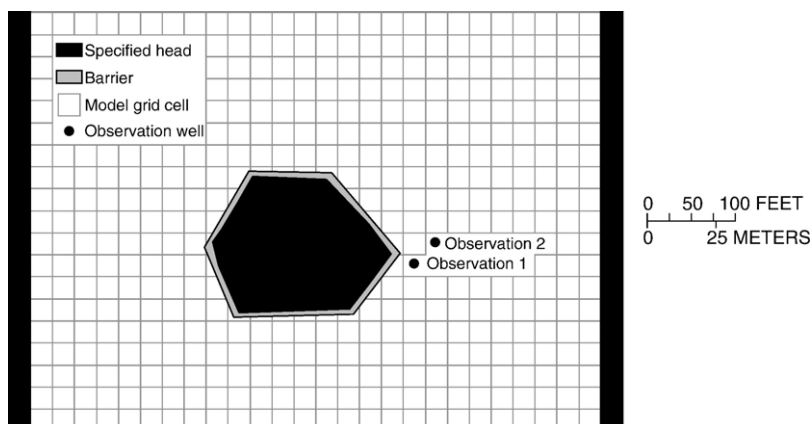


Fig. 4. Hypothetical transport domain with barrier location.

700 ft long in an east–west direction. The thickness of the simulated flow system is 100 ft. Recharge is zero and all flow is derived from the specified-head boundary along the west edge of the flow domain. A 10-ft head difference occurs across the flow system from the specification of heads at the west edge (265 ft) and east edge (255 ft). The northern, southern, and lower boundaries are no-flow. The barrier fully penetrates the aquifer. The area inside the barrier is 27,650 ft².

Because the focus of this work was to assess numerical solutions of the solute transport equation, rather than of the flow equation, a uniform head was specified at nodes interior to the barrier to assure a reasonable head solution. Moderate and reasonable hydraulic gradients were thereby produced between cells inside and outside of the barrier. One of two values of specified head inside the barrier was used in each simulation. A value of 257 ft was used to assure inward gradients around the entire circumference of the barrier. A value of 259 ft was used to produce a slight outward gradient on the downgradient side (east side) of the barrier. Both of these head conditions are similar to observed heads in the field case.

Initial concentrations of PCE were set at 100,000 ppb inside the wall and zero outside the wall. A constant PCE concentration of 100,000 ppb is maintained inside the wall.

A 10-year steady-state flow simulation was run to allow for sufficient time for a constant rate of PCE transport to develop through the wall. The results showed that a steady-state transport of PCE developed 6 months after the start of the simulation.

5.2. Results

Groundwater heads differ by less than 0.1 ft between simulations using the direct and indirect representation of the barrier. Groundwater-velocity vectors also are similar between the direct and indirect methods. Groundwater-flow velocities range from 0.1 to 15 ft/day outside of the barrier. Highest velocities occur where the flow is parallel to the barrier and lowest where the flow is perpendicular to the barrier wall (Fig. 5). Inside the barrier, groundwater velocities are less than 0.05 ft/day.

The two alternative values of specified head inside the barrier either induced an inward gradient around the entire barrier (Fig. 6A) or a slight outward gradient on the downgradient side of the barrier (Fig. 6B). The differences in heads between the two sets of simulations are small and

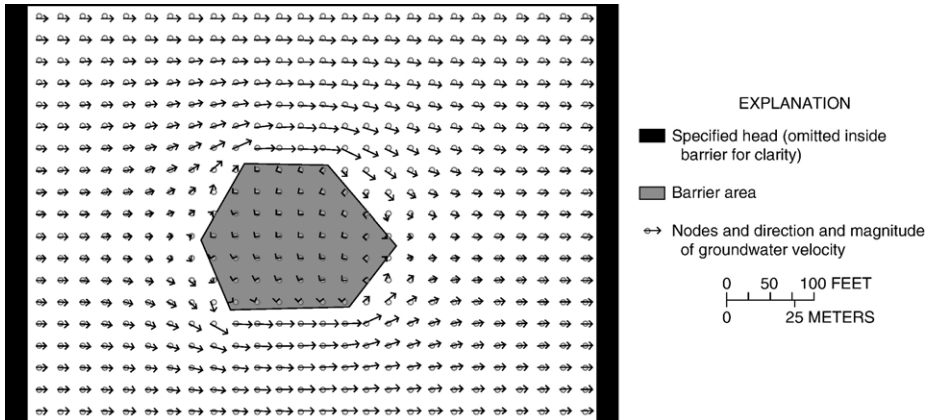


Fig. 5. Horizontal groundwater velocity vectors for the indirect representation of the hypothetical barrier wall (range of velocities 0–15 ft/day).

are limited to areas on the downgradient side of the barrier (Fig. 6A and B; see 258 ft contour is absent in Fig. 6A). There is no outward flow across the barrier for the simulation with the inward gradient (Fig. 6A), and negligible outward flow across the barrier, about $0.8 \text{ ft}^3/\text{day}$ (or 6 gal/day), for the simulation with the outward gradient (Fig. 6B). The small leakage across the barrier for the outward gradient simulation is less than 0.0004% of the total flow across the aquifer.

Model-computed PCE concentrations outside the barrier were tabulated to compare the solute flux through the barrier for several simulations where the barrier was represented by alternative means. PCE concentrations from model runs that simulated the barrier directly (designated with a “D”) and indirectly (designated with a “I”) are listed in Table 1. All simulations presented in Table 1 represent cases with a slight outward gradient (designated as “out”) on the downgradient side of the barrier. (The effect of gradient reversals is discussed below.) Also listed in Table 1 is the model used for the simulation.

Concentrations are reported from the end of the 10-year simulation period for two observation wells located on the downgradient side of the barrier (Fig. 4). The results from the direct representation method show a lower concentration than for the indirect method when the assigned hydraulic-conductivity value of the barrier is assigned to the cell and the width of the barrier is unaccounted for (Table 1; model runs Dout-1 and Dout-2 compared to run Iout-1). However, if the hydraulic conductivity is assigned to the cell based on an equivalent harmonic mean as in Eq. (7), a higher concentration occurs for the direct method (run Dout-3) than for the indirect method (run Iout-1).

The results from simulations with use of the revised code (CHFB package of MODFLOW-GWT) show zero concentrations outside the barrier (Table 1; Iout-2) for the indirect representation method. This demonstrates that all transport of PCE across the barrier using the original code and the indirect representation method was caused by dispersive transport. There is no change in concentrations outside the barrier with the revised code for the direct representation method because cells containing the barrier are treated the same as other model cells (Table 1; runs Dout-2 and Dout-1).

Maps of PCE concentrations from the end of the 10-year simulation period for runs Dout-3, Dout-1, and Iout-1 are shown in Fig. 7. Only values in the range of 0–10 ppb are plotted to more clearly show the distribution of concentrations outside the barrier. Concentrations inside the

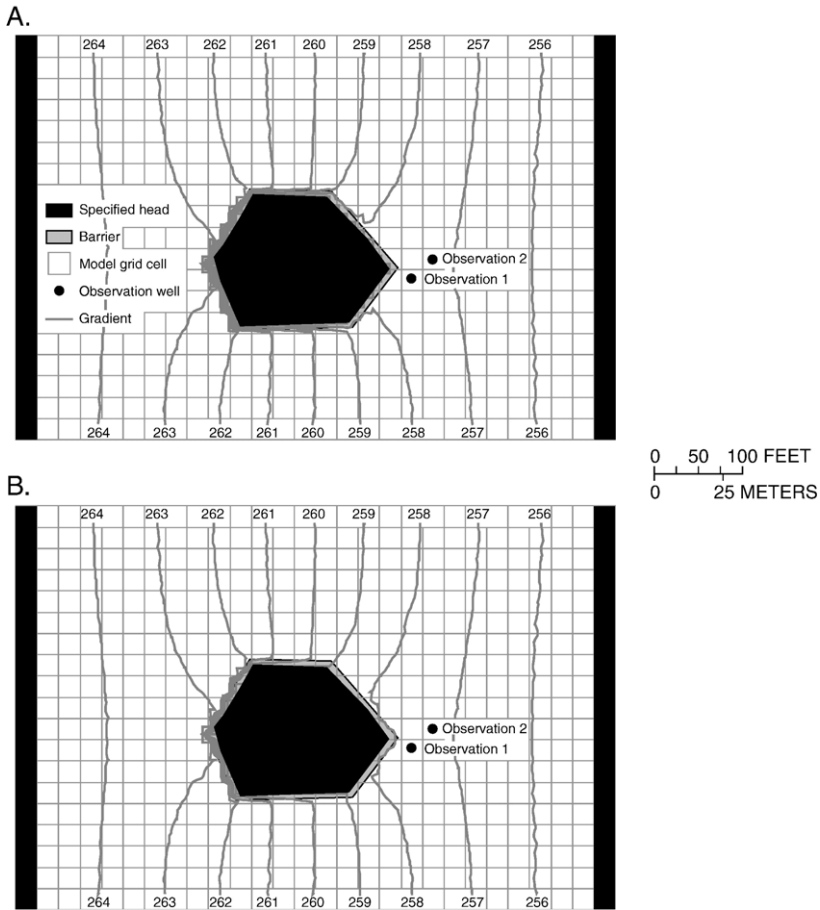


Fig. 6. Groundwater heads, in feet, for inward (A) and outward (B) gradients across the barrier for the hypothetical example.

barrier remain at 100,000 ppb because of the specified boundary conditions. Results show the highest concentration of PCE outside the wall is located on the downgradient side of the barrier for all simulations (Fig. 7). Low concentrations occur on the upgradient side of the barrier and result from dispersive transport against a slight inward advective transport from outside the barrier.

The simulation of the direct representation method, run Dout-1 (Table 1; run Dout-1; Fig. 7B), shows the lowest concentrations outside the barrier. In this simulation, only the barrier hydraulic conductivity is assigned to model cells and the aquifer hydraulic conductivity is ignored although over 80 percent of the cell width is comprised of the aquifer. Therefore, this simulation includes the lowest possible assigned hydraulic conductivity for the model cells containing the barrier and results will tend to underpredict transport rates across the barrier. The simulation is conceptually unrealistic because the hydraulic conductivity of the 3-ft-wide barrier is assigned to the entire 25-ft-wide cell; however, results are useful as an end-member of PCE transport across the barrier.

The simulation of the direct representation, run Dout-3 (Fig. 7A), shows the highest concentrations outside the barrier. For run Dout-3, an equivalent hydraulic conductivity, which

Table 1
Results from hypothetical example of barrier wall^a

Model run no.	Barrier representation type	Gradient direction across barrier	Model	Assigned K_h of cells at barrier (ft/day)	Branch conductance across barrier (ft ² /day)	α_L of barrier (ft)	PCE concentration at 10 years, at observation 1 (ppb)	PCE concentration at 10 years, at observation 2 (ppb)
Dout-1	Direct	Outward	Original	1.42×10^{-4}	2.8×10^{-2}	54.0 (equal to aquifer)	0.5	0.3
Dout-2	Direct	Outward	Revised, no dispersive transport across wall	1.42×10^{-4}	2.8×10^{-2}	0	0.5	0.3
Dout-3	Direct	Outward	Original	1.18×10^{-3}	2.4×10^{-1}	54.0 (equal to aquifer)	4.2	2.3
Iout-1	Indirect	Outward	Original	500	1.1	54.0 (equal to aquifer)	2.6	1.9
Iout-2	Indirect	Outward	Revised, no dispersive transport across wall	500	1.1	0	0	0

^a All model parameter values kept constant except where noted; no., number; K_h is horizontal hydraulic conductivity; α_L is longitudinal dispersivity; barrier K_h is 1.42×10^{-4} ft/day for run Dout-3, K_h is computed from the harmonic mean of the barrier K_h and aquifer K_h ; observation well locations shown on Fig. 4.

includes a proportional assignment of hydraulic conductivities from the aquifer and barrier, is assigned to model cells containing the barrier. Therefore, the hydraulic conductivity at model cells is higher than the hydraulic conductivity at model cells for run Dout-1. As a result, more PCE transport occurs across the barrier and higher PCE concentrations are found outside the barrier.

The simulation of the indirect representation, run Iout-1 (Fig. 7C) shows less PCE transport across the barrier than run Dout-3. Therefore, for a thin barrier relative to the model cell width, the indirect method with use of HFB computes a lower concentration outside the barrier than the direct method that assigns an equivalent hydraulic conductivity to the model cells containing the barrier.

The modification to the transport model in representing barriers with use of the indirect method has correctly reduced dispersive transport across the barrier. The two components in the model that were enhanced included (1) the elimination of the dispersive flux resulting from cross-product terms using erroneous concentration gradients (Eq. (6)) and (2) the ability to designate the barrier with a unique dispersivity value—one that is different than that for the aquifer. In the simulations tested, the dispersivity of the barrier was set to zero. The relative importance of the two modifications is shown in Table 2 for a series of simulations that varied the gradient direction across the barrier.

Use of the modified equation for computing the dispersive flux (Eq. (6)) reduces dispersive transport across the barrier in the test problem by approximately 50% (Table 2). PCE is measurable under both hydraulic gradient conditions suggesting that dispersive flux will occur from concentration gradients regardless of the advective transport direction under low velocity

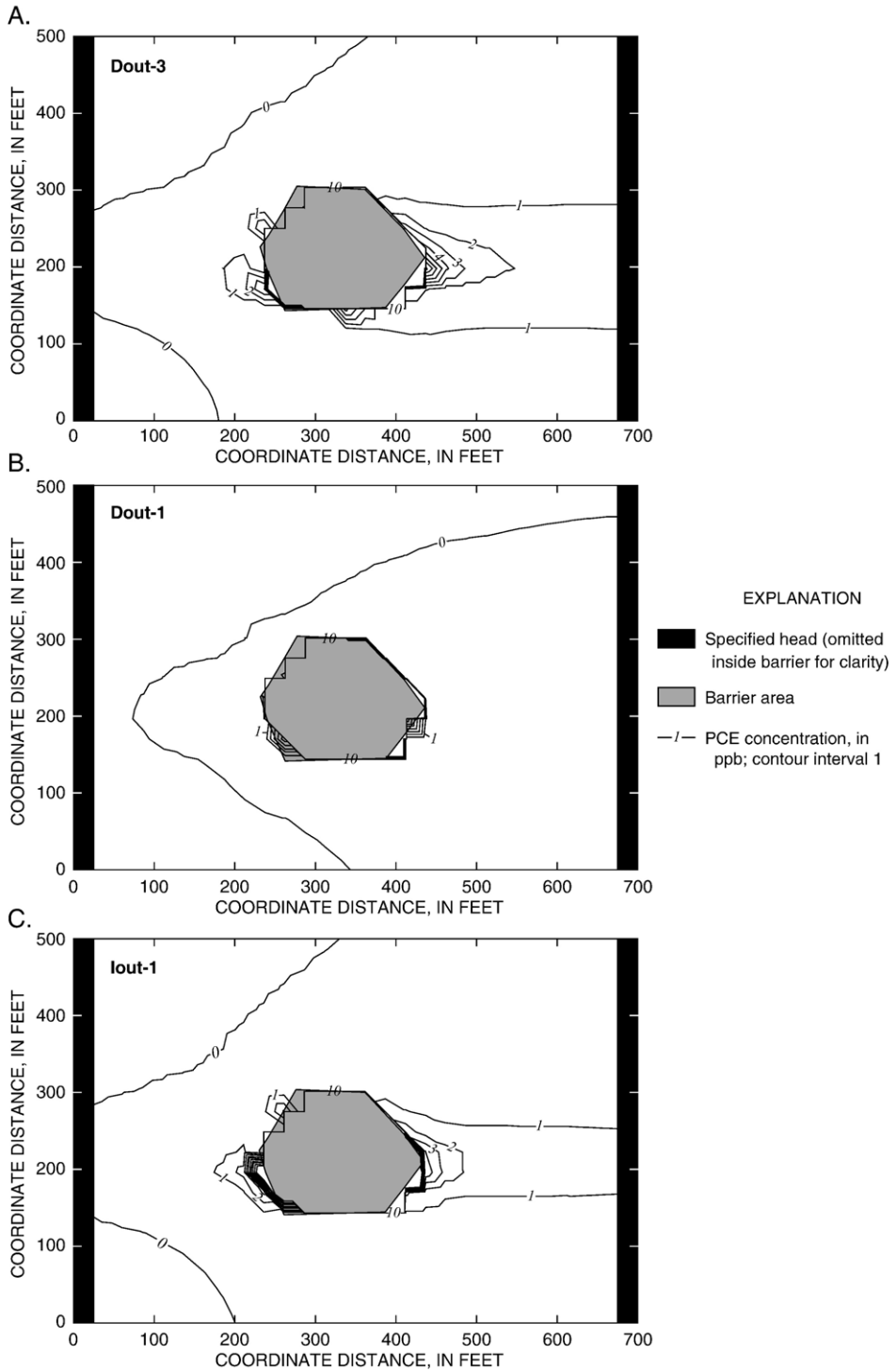


Fig. 7. Contours of equal concentration of PCE in ppb for direct runs Dout-3 (A) and Dout-1 (B) and indirect run Iout-1 (C) representation methods of the barrier for the hypothetical example.

Table 2

Simulated PCE concentrations (ppb) at observation well 1 from indirect representation of barrier wall in a hypothetical example

Gradient direction across barrier	Barrier dispersivity=aquifer		Barrier dispersivity=0
	Original dispersive flux (Eq. (5))	Modified dispersive flux (Eq. (6))	
Inward	1.8	1.2	0.1
Outward	3.6	2.2	0.1

conditions. Assigning a value of zero for dispersivity of the barrier essentially eliminates dispersive transport for either gradient scenario.

The focus of model simulations involved testing the effect of alternate methods in representing a low-permeability, horizontal-flow barrier on solute transport. Other factors were tested but not presented in this paper including model cell size, and the amount of flow through the aquifer system. Both factors (cell size and flow) affected the slow velocity zone downgradient of the barrier and impacted concentrations of PCE outside the barrier. Therefore, these factors should be evaluated along with the representation methods discussed in this paper.

6. Field case

6.1. Description

The field case is the Savage Municipal Well Superfund site in Milford, New Hampshire (Fig. 8). The site is underlain by a large (0.5 mi^2) and thick (100 ft) primarily PCE volatile organic plume. The primary source area of the PCE contamination was a tool manufacturing facility (HMM Associates, Inc., 1991) located in the western part of a valley-fill, glacially deposited aquifer. The tool company discharged solvents into the subsurface for many years until the early 1980s. Although discharges had ceased after closure of the tool company, the underlying contaminant-soaked sediments and pockets of immiscible solvents continued to contaminate groundwater flowing easterly underneath the site until a barrier wall was constructed in 1998–1999.

The field case incorporates aquifer heterogeneity, groundwater recharge from infiltration of precipitation and river leakage, and injection (including a recharge gallery) and extraction wells, and transient groundwater flow. The barrier is only simulated indirectly with the HFB Package.

Groundwater flow is to the east at velocities of up to several ft/day in unconsolidated, sand and gravel sediments of the aquifer. A partially penetrating river, the Souhegan River, bounds the northwestern part of the source area. The river recharges the aquifer at an average rate of about $4 \text{ ft}^3/\text{s}$ (Harte et al., 1997) and is simulated as a specified-head boundary with recharge rates calculated based on the gradient between the river stage and aquifer head for an assigned riverbed conductance. Flowpaths from the river are tangential to the river in a west to east direction (Fig. 8A). Groundwater recharge from infiltration of precipitation ranges from about 12 in./year inside the barrier because of a partial land-surface cap to 24 in. outside the barrier (Brayton and Harte, 2001). Additional information on groundwater flow at this site can be found in Harte and Willey (1997) and Harte et al. (1999).

The barrier wall is constructed of low-permeability, bentonite slurry, which was emplaced by trenching. The barrier wall encapsulates the highest concentrations of contaminants and

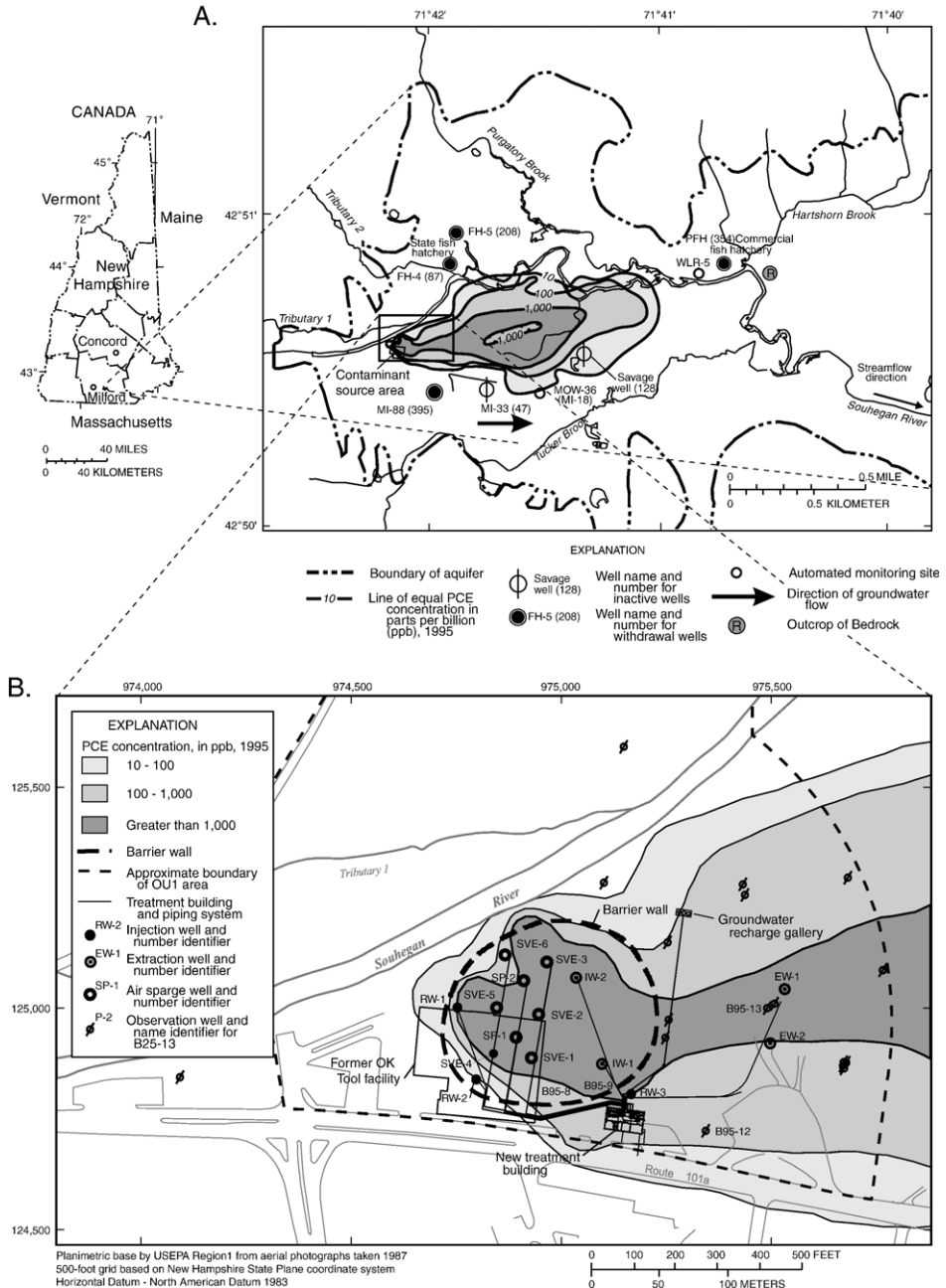


Fig. 8. Location of field case of barrier wall in New Hampshire, (A) the valley fill, glacially deposited aquifer and PCE plume in which it occurs and (B) map of source area with remedial design.

encloses an area of about 220,000 ft². The barrier primarily penetrates the full thickness of the sand and gravel unit and parts of a basal till and sits primarily atop the underlying bedrock.

Injection (RW) and extraction (IW and EW) wells (Fig. 8B) were installed inside and outside the barrier in the unconsolidated sediments. Remedial wells inside the barrier are used to hydraulically isolate the contaminants inside the barrier and to reduce the mass of contaminants. Remedial wells outside the barrier are used to capture contaminants outside the barrier by reducing contaminant mass and capturing contaminants that may leak through the barrier (Camp et al., 1996). Extraction rates range from about 9 gal/min for interior (IW) wells to 25 gal/min for exterior (EW) wells.

PCE is the primary contaminant and its maximum concentrations range from 100,000 ppb inside the wall to 10,000 ppb outside the wall. Concentrations of secondary VOC contaminant (TCE and *cis*-1,2,DCE) are typically one to two orders of magnitude less than those of PCE and are not simulated. Unlike the hypothetical example, there is no additional input of PCE after the initial starting conditions and PCE occurs outside the barrier as a starting condition.

The model of the field case consists of over 33,000 cells and covers the area shown in Fig. 8A. In the contaminant source area (Fig. 8), it contains about 3000 cells (Fig. 9). The angle of the grid is aligned with the predominant groundwater flow direction (southwest–northeast). The model consists of five layers, each about 20 ft thick except for the lowermost layer, which is slightly thicker or thinner depending on the total depth of the aquifer. The extent of the solute grid (subgrid) is smaller than the model grid (Fig. 10) to reduce computational time.

The simulated flow system includes all unconsolidated sediments above the simulated no-flow boundary at the bedrock surface. The unconsolidated sediments are simulated as heterogeneous and anisotropic. The hydraulic conductivity varied from 15 to 450 ft/day horizontally and 4 to 112 ft/day vertically (1/4 the horizontal). In this paper, representative results are provided from grid layers three (middle layer) and five (lowermost layer).

The simulation time period exceeded 40 years to allow for sufficient time to reduce contaminant concentrations outside the barrier to below 5 ppb (the remediation goal). The simulations assume transient-flow conditions with constant rates of extraction and injection, recharge, and values of river stage per stress period. Two principal stress periods were simulated

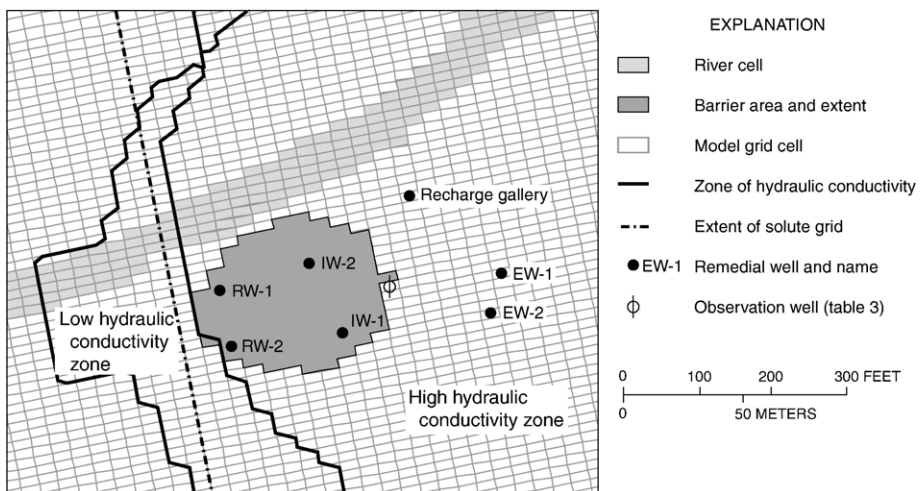


Fig. 9. Model grid of source area, barrier, remedial wells, river, and hydraulic conductivity zones (middle layer 3) for field case.

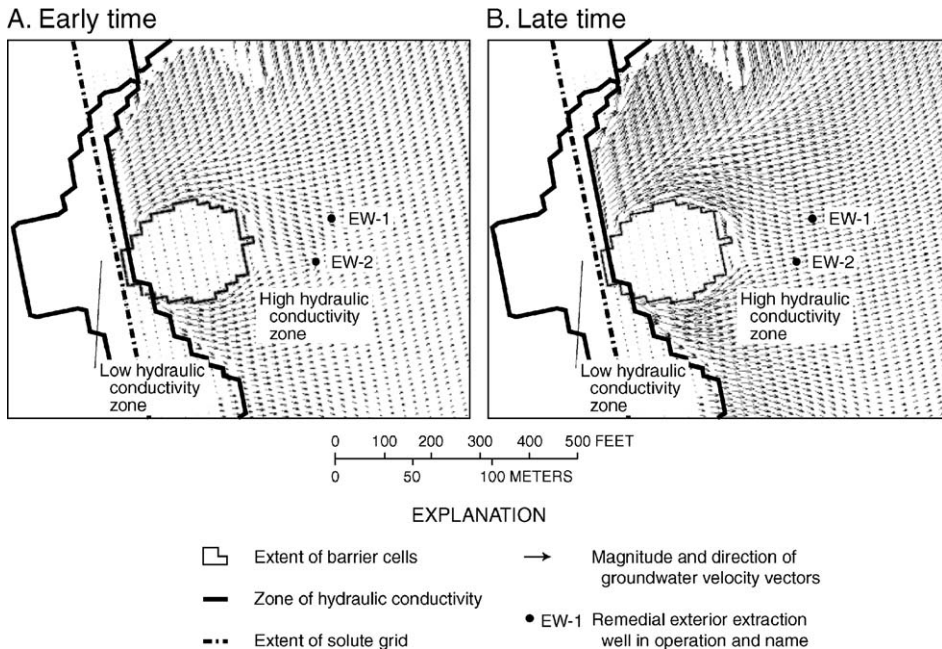


Fig. 10. Horizontal groundwater velocity vectors in layer 3 of grid for indirect representation of barrier from field case (range of velocities 0.03–3.0 ft/day) for (A) remedial operation of exterior extraction well and (B) no operation of exterior extraction well.

and included a 6-year period of operational remedial wells and a 24-year period of operational interior (inside the barrier) remedial wells but discontinued exterior (outside) extraction wells. The impact of discontinuing exterior extraction operations is evaluated.

6.2. Results

Horizontal groundwater velocities range from less than 0.03 ft/day to more than 3 ft/day (Fig. 10). Velocities are affected by the barrier, variations in hydraulic conductivity, and injection and extraction from remedial wells. Computed horizontal groundwater velocity vectors in the layer 3 of the aquifer for two time periods (early and late) are shown in Fig. 10. During the early simulation time (Fig. 10A), remedial extraction wells outside the barrier are in operation and flow vectors are toward the exterior extraction wells. Downgradient of the wells, flow is slow from a creation of a stagnation zone in the “shadow of the capture zone.” At later times (Fig. 10B), the exterior wells are shut off and flow vectors become relatively uniform and flow is no longer reduced downgradient of the extraction wells.

Similar to the hypothetical example, the highest groundwater velocities occur outside the barrier where the flow is parallel to the barrier wall and lowest where the flow is perpendicular to the barrier wall. Slow velocity zones occur on the upgradient and downgradient side of the barrier. Differences in velocities also are caused by the two assigned hydraulic-conductivity zones (15 ft/day and 150 ft/day) in the middle layer (3). A river boundary is partially penetrating and overlies the middle layer of the simulated aquifer that is shown in Fig. 10. Flow under the river is parallel to the direction of the streamflow (southwest to northeast). Inside the barrier, flow is slow because

the barrier reduces flow into and out of the interior barrier area and injection and extraction rates of remedial wells are small (less than 10 gal/min).

A key objective of the solute-transport simulations was to quantify the transport of PCE through the barrier and its effect on the remediation of PCE outside the barrier. There are two important distinctions between the hypothetical example and the field case: (1) for the field case, PCE is initially present outside of the barrier, and (2) for the field case, no additional input of PCE is added inside the barrier after the start of the simulation.

Model-computed PCE transport through the barrier affects concentrations outside the barrier for many years, as illustrated in Fig. 11 for an observation well located next to extraction well EW-1 (Fig. 8B). Two simulations were performed to examine PCE transport through the barrier. The first simulation specified initial PCE concentrations inside the barrier similar to concentrations observed in the field, and the second specified no PCE (initial PCE concentration of zero) inside the barrier. Simulations were made with the original MODFLOW-GWT code. The differences in model simulations reflect the impact of slow PCE transport through the wall under the first scenario. In this case, PCE concentrations inside the barrier initially are much higher than PCE concentrations outside the barrier, and solute flux across the barrier over time produces a tailing phenomenon that can prolong remediation efforts outside the barrier. The tailing problem will persist for a very long time because the barrier slows the rate of flushing inside the barrier.

Extraction wells EW-1 and EW-2 are located outside the barrier (Fig. 8B) and were simulated until year 6. A small increase in calculated PCE concentrations occurs after these extraction wells are turned off (Fig. 11) because of a reduction in dilution of vertical flow and transport of relatively low PCE concentration waters from shallow model layers (1–3). PCE transport through the barrier increases PCE concentrations outside the barrier for a continued period as shown by the differences in PCE declines (Fig. 11) between the two simulations.

Differences in PCE concentrations directly outside the barrier are smallest in the early times of the simulation (Table 3) but increase in the latter stages of the simulation. Table 3 lists calculated PCE concentrations for a model cell located outside the barrier (Fig. 9) and shows the difference in concentrations from simulations with and without the initial presence of PCE inside the wall.

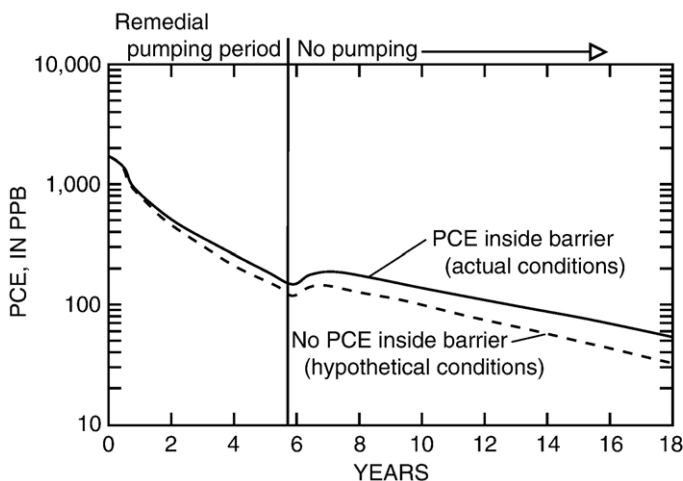


Fig. 11. PCE concentration declines from an observation well (B95-13, Fig. 8B) next to extraction well EW-1 from field case.

Table 3

Results from field case simulation using HFB Package to indirectly represent the barrier with and without PCE initially present inside the barrier

Time, in years, from beginning of simulation	Simulation ^a with initial PCE assigned inside barrier, concentration in ppb	Simulation ^a with no initial PCE assigned inside barrier, concentration in ppb	Relative percent difference
0	1736	1736	0
1	1730	1629	6
6	1198	999	18.1
10	1045	865	18.8
15	886	725	20
26	606	481	22.9
46	263	204	25.3

^a PCE concentration in ppb from model cell located directly outside the barrier wall; location shown on Fig. 9.

The relative percent difference between calculated concentrations increases with time. These results are consistent with the occurrence of dispersive transport across the barrier. PCE flux from dispersive transport across the barrier is relatively slower during the early times of the simulation than the later times because the concentration gradient increases with time due to differential rates of flushing inside and outside the barrier.

A simulation with the revised MODFLOW-GWT code using Eq. (6) was run for the field case (base condition with initial PCE concentrations inside the barrier) to quantify PCE flux through the barrier from dispersive transport. A dispersivity of 1/10 the aquifer dispersivity was assigned

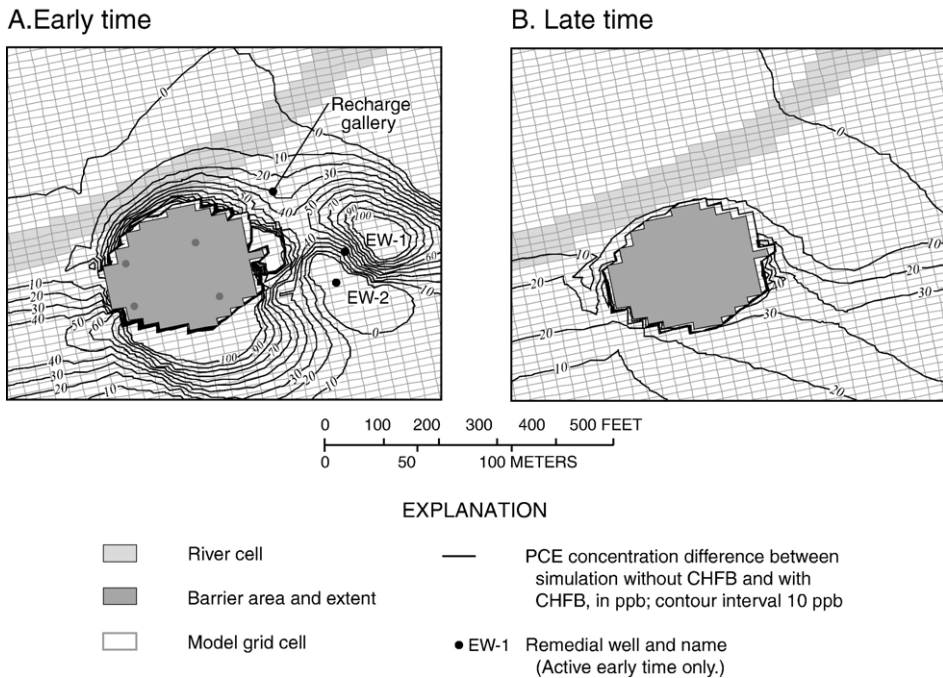


Fig. 12. Contours of PCE concentration differences between simulations without and with use of CHFB Package for model layer 3 for (A) early time and (B) late time simulation.

to the barrier. Concentration differences from results of simulations without and with use of revised code (CHFB Package of MODFLOW-GWT) were plotted from model layer 3 for two time periods (early and late). The remedial extraction wells outside the barrier are operational during the early simulation time (Fig. 12A), but not during the late simulation time (Fig. 12B).

The revised MODFLOW-GWT code computes lower PCE concentrations outside the barrier than did the original code. This indicates there is less dispersive transport through the barrier when the dispersive flux equation (Eq. (6)) is modified and the dispersivity values for the barrier are decreased from the aquifer dispersivity. For early time, differences exceed 100 ppb (Fig. 12A) and for late time, differences are less than 40 ppb (Fig. 12B). The PCE concentration outside the barrier, for the simulation using CHFB, primarily represents PCE from two sources: (1) a small amount of PCE transported across the barrier by advection and (2) residual PCE from outside the barrier before the start-up of remediation and barrier emplacement. As a result of the decreased dispersive transport through the barrier, PCE concentrations inside the barrier (not shown) are higher (by approximately 500 ppb) during the late simulation time with the revised code than with the original code. Consequently, the new CHFB Package indicates that PCE transport through the barrier will occur at a lower magnitude and rate at early times, but that PCE transport will persist for a longer duration and lead to a slower tailing process than that computed with the original code.

7. Conclusions

Direct representation of low-permeability, barrier walls in numerical models is advantageous if the hydraulic properties of the barrier can be accurately assigned to the model cells where the barrier is located. To be accurate, the dimensions of the barrier must be similar to the dimensions of the model cells where it is located, which may require an extremely fine and, consequently, impractical model grid. The assignment of the hydraulic properties of a narrow barrier to a relatively wide model cell will produce an equivalent hydraulic property unrepresentative of the hydraulic properties of the barrier or of the aquifer. In the example provided in this paper, a barrier wall 20% of the width of the model cell size yielded an equivalent hydraulic conductivity that was six times greater than the hydraulic conductivity of the barrier. The simulation using this equivalent hydraulic conductivity yielded higher transport of PCE through the barrier than was produced using an indirect representation method.

If a horizontal-flow barrier is indirectly represented, such as by using the HFB Package of MODFLOW, then the standard finite-difference formulation for estimating concentration gradients may yield overestimates in solute transport through barriers by assuming smooth or linear transitions in concentration differences between cells on opposite sides of the barrier. This normally reasonable assumption may fail in the vicinity of a barrier because the barrier, by its very nature or design, represents a discontinuity in composition and hydraulic properties. A revised equation is used to compute concentration gradients, which drive dispersion, separately, on opposite sides of the barrier, by only considering concentrations for nodes on a single side of a barrier as a driving force for dispersive fluxes on that side of the barrier. This new formulation, coupled with the ability to specify dispersive properties for the barrier that differ from those of the aquifer (incorporated into the CHFB Package of MODFLOW-GWT), resulted in reduced dispersive transport of PCE across a barrier in both the hypothetical and field problems simulated in this study. These results are believed to be more reliable and accurate than those obtained with conventional dispersion solutions. The reduction in PCE flux calculated using CHFB with MODFLOW-GWT indicated that most of the simulated transport across the low-permeability

barrier originated from dispersive transport and not from advective transport through the barrier. The effects of the barrier on groundwater flow can be efficiently simulated when the barrier is represented indirectly, such as by using the HFB Package in MODFLOW. However, if solute transport is simulated simultaneously, then the dispersive flux across the barrier should be calculated using a modified equation that recognizes and accounts for a potentially sharp discontinuity in the concentration field at the location of the barrier coincident with a cell face.

References

- Borowiec, Jr., P.J., 1998. Letter on soil bentonite barrier wall properties, OK Tool/Savage Municipal Well Superfund Site, Milford, New Hampshire: Camp, Dresser, and McKee, Inc., Cambridge, Mass., 1 p.
- Brayton, M.J., Harte, P.T., 2001. Results of a monitoring program of continuous water levels, specific conductance, and water temperature at the OK Tool facility of the Savage Municipal Well Superfund site, Milford, New Hampshire: U.S. Geol. Survey Open-File Report 01-338, 50 pp.
- Camp, Dresser, McKee, Inc., 1996. Conceptual Remedial Design Report, Volume 1, for OK Tool Source Area, Savage Municipal Supply Well, Superfund Site-OU1, Milford, New Hampshire: CDM Inc., 10 Cambridge Center, Cambridge, Mass., March 1996, vol. 1, 5 chaps.
- Harbaugh, A.W., McDonald, M.G., 1996. User's documentation for MODFLOW-96, an update to the U.S. Geological Survey modular finite-difference ground-water flow model: U.S. Geol. Survey Open-File Report 96-485, 56 pp.
- Harbaugh, A.W., Banta, E.R., Hill, M.C., McDonald, M.G., 2000. MODFLOW-2000, The U.S. Geological Survey modular ground-water model—User guide to modularization concepts and the ground-water flow process: U.S. Geol. Survey Open-File Report 00-92, 121 pp.
- Harte, P.T., Willey, R.E., 1997. Effects of historical withdrawals on advective transport of contaminated ground waters in a glacial-drift aquifer, Milford, New Hampshire; U.S. Geol. Survey Factsheet 162-97, 6 pp.
- Harte, P.T., Flynn, R.H., Kiah, Richard, Severance, Timothy, Coakley, M.F., 1997. Information on hydrologic and physical properties of water to assess transient hydrology of the Milford-Souhegan glacial-drift aquifer, Milford, New Hampshire: U.S. Geol. Survey Open-File Report 97-414, 96 pp.
- Harte, P.T., Flynn, R.H., Mack, T.J., 1999. Construction and calibration of numerical ground-water flow models of the western half of the Milford-Souhegan Glacial-Drift Aquifer, Milford, New Hampshire: U.S. Geol. Survey Open-File Report 99-462, 76 pp.
- Heberton, C.I., Russell, T.F., Konikow, L.F., Hornberger, G.Z., 2000. A three-dimensional finite-volume Eulerian-Lagrangian localized adjoint method (ELLAM) for solute-transport modeling: U.S. Geol. Survey Water-Resources Investigations Report 00-4087, 63 pp.
- HMM Associates, Inc., 1991. Remedial investigation, Savage well site, Milford, New Hampshire: Concord, Mass., no. 2176 HAZ/4814, 800 pp.
- Hornberger, G.Z., Konikow, L.F., Harte, P.T., 2002. Simulating solute transport across horizontal-flow barriers using the MODFLOW Ground-Water Transport Process: U.S. Geol. Survey Open-File Report 02-52, 28 pp.
- Hsieh, P.A., Freckleton, J.R., 1993. Documentation of a computer program to simulate horizontal-flow barriers using the U.S. Geological Survey's modular three-dimensional finite-difference ground-water flow model: U.S. Geol. Survey Open-File Report 92-477, 32 pp.
- Kipp, Jr., K.L., Konikow, L.F., Hornberger, G.Z., 1998. An implicit dispersive transport algorithm for the U.S. Geological Survey MOC3D solute-transport model: U.S. Geol. Survey Water-Resources Investigations Report 98-4234, 54 pp.
- Knox, R.C., Canter, L.W., Kincannon, D.F., Stover, E.L., Ward, C.H., 1984. State-of-the art of aquifer restoration, EPA/600/2-84/182a and b (National Technical Information Service [NTIS]PB85-181071 and PB85-181089), R.S. Kerr Environmental Research Laboratory, Ada, OK.
- Konikow, L.F., Goode, D.J., Hornberger, G.Z., 1996. A three-dimensional method of characteristics solute-transport model (MOC3D): U.S. Geol. Survey Water-Resources Investigations Report 96-4267, 87 pp.
- Konikow, L.F., Harte, P.T., Hornberger, G.Z., 2001. Simulating solute transport across horizontal-flow barriers. In: Seo, H. S., Poeter, E., Zheng, C., Poeter, O. (Eds.), MODFLOW 2001 and Other Modeling Odysseys, International Ground Water Modeling Center, Golden, CO, pp. 510–516.
- McDonald, M.G., Harbaugh, A.W., 1988. A modular three-dimensional finite-difference ground-water flow model: U.S. Geol. Survey Techniques of Water-Resources Investigations, book 6, chap. A1, 586 pp.

- Neville, C.J., Riley, M.J., Zheng, C., 1998. Implicit modeling of low permeability features: an appraisal for solute transport. In: Poeter, E., Zheng, C., Hill, M. (Eds.), MODFLOW 98 Proceedings, vol. 1. Colorado School of Mines, Golden, Co., pp. 353–362.
- U.S. Environmental Protection Agency, 1996. Pump-and-treat ground-water remediation. A Guide for Decision Makers and Practitioners: U.S. Environmental Protection Agency. Office of Research and Development, Cincinnati, OH. 73 pp.